We selected STI571 because this compound is known to target the PDGF-R TK (see Introduction). NP-incorporated with STI571 attenuated the proliferation of human VSMCs in vitro and the formation of vein graft neointima formation in vivo, both of which are known to be associated with the inhibition of the target molecules of STI571 (PDGF-R TK, c-Abl TK) and downstream signal of PDGF-R (ERK). NP-incorporated with STI571 did not affect endothelial regeneration process after vein grafting. In preliminary experiments, tissue concentrations of STI571 were measured immediately after and 6 hours after incubation of excised veins with STI571-NP by HPLC system, which showed under the limit of detection (1 ng/mL). Although the precise intracellular concentration and distribution of STI571 is unclear, our present data (Figures 2 and 4) provide evidence that (1) STI571-incorporated NP may block PDGF-R signaling possibly via slow release of STI-571 into the cytoplasm as NP is hydrolyzed; and (2) PDGF-R signaling blockade by NP-incorporated with STI571 is a means for treating vein graft neointima formation in vivo.

Inflammatory-proliferative changes have been shown to play a central role in the pathogenesis of vein graft neointima formation. In early stages, the neointima lesion has an inflammatory nature characterized by mononuclear cell infiltration, followed by VSMC proliferation.[19] We recently reported that blockade of monocyte chemoattractant protein-1 (MCP-1) by adenovirus-mediated ex vivo transfer of 7ND gene to autologous vein grafts suppressed neointima formation in dogs.[18] We also have demonstrated that MCP-1 plays a central role in neointima formation following arterial mechanical injury.[20,21,22] In a previous study,[18] we showed that blockade of MCP-1 attenuated both inflammation (monocyte infiltration) and proliferation (appearance of proliferating VSMC) in vein grafts. In contrast, data from this study show that NP-mediated delivery of STI571 reduced PDGF-induced proliferation but not inflammation, suggesting that (1) PDGF-mediated proliferative changes might be located downstream of inflammatory changes, or (2) the mechanism of action of STI571-mediated inhibition of proliferation might be distinct from that of anti-MCP-1-mediated attenuation of proliferation and inflammation. If STI571 and anti-MCP-1 treatment exert their effects through different pathways, it would be interesting to examine whether combined blockade of PDGF and MCP-1 would have additive inhibitory effects on vein graft failure.

Expression of PDGF is known to be low in normal blood vessels, but mechanical forces stimulate SMC expression and release of PDGF, and induce PDGF-R phosphorylation (activation).[23] We show here that PDGF and the phosphorylation levels of its receptor were up-regulated in vein grafts. STI571-incorporated NP did not affect increased PDGF expression, but it did suppress the protein expression of PDGF-R, PDGF-R kinase, and c-Abl TK in vivo. This could suggest the presence of a positive-feedback loop that, in the absence of STI571, potentiates PDGF-mediated proliferation in vein grafts. It is also possible that reduced PDGF-producing cells (PCNA-positive cells) in the vein graft or blockade of multiple intracellular kinases might have contributed to the beneficial effects of STI571-incorporated NP on vein graft neointima formation in vivo.

One limitation in the present study is that only single dose of STI571-NP was examined. It is practically difficult to obtain the dose–response relationship of this NP system in small animals, because the dose–response relation of STI571 and polymer needs to be examined. For translation of our present findings into clinical medicine, further studies are therefore needed to define a dose-response relation in large animal models.

In conclusion, blockade of PDGF signaling by STI571-incorporated NP-inhibited proliferation of VSMCs in vitro and suppressed vein graft neointima formation in vivo. This NP-mediated drug delivery system provides an innovative and clinically feasible therapeutic strategy for preventing vein graft failure.

Sources of Funding

This study was supported by Grants-in-Aid for Scientific Research (19390216, 19650134) from the Ministry of Education, Science, and Culture, Tokyo, Japan and by Health Science Research Grants (Research on Translational Research and Nano-medicine) from the Ministry of Health Labor and Welfare, Tokyo, Japan.

Disclosures

Dr Egashira holds a patent on the results reported in the present study. The other authors report no conflicts.

References

1. Fitzgibbon GM, Kafka HP, Leach AJ, Keon WJ, Hooper GD, Burton JR. Coronary bypass graft fate and patient outcome: angiographic follow-up of 5,065 grafts related to survival and reoperation in 1,388 patients during 25 years. *J Am Coll Cardiol.* 1996;28:616–626.
2. Schachner T, Laufer G, Bonatti J. In vivo (animal) models of vein graft disease. *Eur J Cardiothorac Surg.* 2006;30:451–463.
3. Savage DG, Antman KH. Imatinib mesylate–a new oral targeted therapy. *N Engl J Med.* 2002;346:683–693.
4. Sata M, Saiura A, Kunisato A, Tojo A, Okada S, Tokuhisa T, Hirai H, Makuuchi M, Hirata Y, Nagai R. Hematopoietic stem cells differentiate into vascular cells that participate in the pathogenesis of atherosclerosis. *Nat Med.* 2002;8:403–409.
5. Ushio-Fukai M, Zuo L, Ikeda S, Tojo T, Patrushev NA, Alexander RW. cAbl tyrosine kinase mediates reactive oxygen species- and caveolin-dependent AT1 receptor signaling in vascular smooth muscle: role in vascular hypertrophy. *Circ Res.* 2005;97:829–836.
6. Hacker TA, Griffin MO, Guttormsen B, Stoker S, Wolff MR. Platelet-Derived Growth Factor Receptor Antagonist STI571 (Imatinib Mesylate) Inhibits Human Vascular Smooth Muscle Proliferation and Migration In Vitro but Not In Vivo. *J Invasive Cardiol.* 2007;19:269–274.
7. Myllarniemi M, Frosen J, Calderon Ramirez LG, Buchdunger E, Lemstrom K, Hayry P. Selective tyrosine kinase inhibitor for the platelet-derived growth factor receptor in vitro inhibits smooth muscle cell proliferation after reinjury of arterial intima in vivo. *Cardiovasc Drugs Ther.* 1999;13:159–168.
8. Leppanen O, Rutanen J, Hiltunen MO, Rissanen TT, Turunen MP, Sjoblom T, Bruggen J, Backstrom G, Carlsson M, Buchdunger E, Bergqvist D, Alitalo K, Heldin CH, Ostman A, Yla-Herttuala S. Oral imatinib mesylate (STI571/gleevec) improves the efficacy of local intravascular vascular endothelial growth factor-C gene transfer in reducing neointimal growth in hypercholesterolemic rabbits. *Circulation.* 2004; 109:1140–1146.
9. Zohlnhofer D, Hausleiter J, Kastrati A, Mehilli J, Goos C, Schuhlen H, Pache J, Pogatsa-Murray G, Heemann U, Dirschinger J, Schomig A. A randomized, double-blind, placebo-controlled trial on restenosis prevention by the receptor tyrosine kinase inhibitor imatinib. *J Am Coll Cardiol.* 2005;46:1999–2003.
10. Peng B, Hayes M, Resta D, Racine-Poon A, Druker BJ, Talpaz M, Sawyers CL, Rosamilia M, Ford J, Lloyd P, Capdeville R. Pharmacoki-

netics and pharmacodynamics of imatinib in a phase I trial with chronic myeloid leukemia patients. *J Clin Oncol.* 2004;22:935–942.
11. Kerkela R, Grazette L, Yacobi R, Iliescu C, Patten R, Beahm C, Walters B, Shevtsov S, Pesant S, Clubb FJ, Rosenzweig A, Salomon RN, Van Etten RA, Alroy J, Durand JB, Force T. Cardiotoxicity of the cancer therapeutic agent imatinib mesylate. *Nat Med.* 2006;12:908–916.
12. Murakami H, Kobayashi M, Takeuchi H, Kawashima Y. Preparation of poly(DL-lactide-co-glycolide) nanoparticles by modified spontaneous emulsification solvent diffusion method. *Int J Pharm.* 1999; 187:143–152.
13. Kawashima Y, Yamamoto H, Takeuchi H, Hino T, Niwa T. Properties of a peptide containing DL-lactide/glycolide copolymer nanospheres prepared by novel emulsion solvent diffusion methods. *Eur J Pharm Biopharm.* 1998;45:41–48.
14. Rejman J, Oberle V, Zuhorn IS, Hoekstra D. Size-dependent internalization of particles via the pathways of clathrin- and caveolae-mediated endocytosis. *Biochem J.* 2004;377:159–169.
15. Panyam J, Zhou WZ, Prabha S, Sahoo SK, Labhasetwar V. Rapid endolysosomal escape of poly(DL-lactide-co-glycolide) nanoparticles: implications for drug and gene delivery. *Faseb J.* 2002;16:1217–1226.
16. Nakano K, Egashira K, Tada H, Kohjimoto Y, Hirouchi Y, Kitajima S, Endo Y, Li XH, Sunagawa K. A third-generation, long-acting, dihydropyridine calcium antagonist, azelnidipine, attenuates stent-associated neointimal formation in non-human primates. *J Hypertens.* 2006;24: 1881–1889.
17. Chen Z, Lee FY, Bhalla KN, Wu J. Potent inhibition of platelet-derived growth factor-induced responses in vascular smooth muscle cells by BMS-354825 (dasatinib). *Mol Pharmacol.* 2006;69:1527–1533.
18. Tatewaki H, Egashira K, Kimura S, Nishida T, Morita S, Tominaga R. Blockade of monocyte chemoattractant protein-1 by adenoviral gene transfer inhibits experimental vein graft neointimal formation. *J Vasc Surg.* 2007;45:1236–1243.
19. Motwani JG, Topol EJ. Aortocoronary saphenous vein graft disease: pathogenesis, predisposition, and prevention. *Circulation.* 1998;97: 916–931.
20. Usui M, Egashira K, Ohtani K, Kataoka C, Ishibashi M, Hiasa K, Katoh M, Zhao Q, Kitamoto S, Takeshita A. Anti-monocyte chemoattractant protein-1 gene therapy inhibits restenotic changes (neointimal hyperplasia) after balloon injury in rats and monkeys. *Faseb J.* 2002;16: 1838–1840.
21. Egashira K, Zhao Q, Kataoka C, Ohtani K, Usui M, Charo IF, Nishida K, Inoue S, Katoh M, Ichiki T, Takeshita A. Importance of monocyte chemoattractant protein-1 pathway in neointimal hyperplasia after periarterial injury in mice and monkeys. *Circ Res.* 2002;90:1167–1172.
22. Ohtani K, Usui M, Nakano K, Kohjimoto Y, Kitajima S, Hirouchi Y, Li XH, Kitamoto S, Takeshita A, Egashira K. Antimonocyte chemoattractant protein-1 gene therapy reduces experimental in-stent restenosis in hypercholesterolemic rabbits and monkeys. *Gene Ther.* 2004;11: 1273–1282.
23. Wilson E, Mai Q, Sudhir K, Weiss RH, Ives HE. Mechanical strain induces growth of vascular smooth muscle cells via autocrine action of PDGF. *J Cell Biol.* 1993;123:741–747.

Online Data Supplements

Materials and Methods

Preparation of PEG-PLGA NP

STI571 (a PDGF-R tyrosine kinase inhibitor, Novartis) was purchased from pharmacy. A poly-(ethylene glycol)-*block*-lactide/glycolide copolymer (PEG-PLGA) with an average molecular weight of 22,900 and a PLGA copolymer ratio of lactide to glycolide of 75:25 (Absorbable Polymers International,USA) was used as a wall material for the NP. Fluorescein-isothiocyanate (FITC, Dojindo laboratories, Kumamoto, Japan) and coumarin-6 (MP Biomedicals) were used as fluorescent markers of the NP.

The fluorescence markers and the STI571-encapsulated PEG-PLGA NP was prepared using an emulsion solvent diffusion method, as previously reported.[1, 2] These three ingredients to be encapsulated in PEG-PLGA were prepared separately. Both 0.1 g of FITC and 0.001 g of coumarin-6 as fluorescence marker were dissolved in a 10 ml ethanol solution respectively and then, mixed with a 20 ml acetone solution containing 2.0 g of PEG-PLGA. Also 0.3 g of STI571 was dissolved in a 10 ml methanol solution and mixed a 20 ml acetone solution containing 2.0 g of PEG-PLGA. Each one of the solutions was dropped into 50 ml purified water at 40 °C with a speed of 400 rpm using the propeller-type agitator with four blades. After evaporating the organic solvent for about 2 hours under reduced pressure at 40 °C, the prepared suspension of the fluorescence markers or the STI571- encapsulated PEG-PLGA NP was filtrated using a membrane filter having 32 μm in average pore size for removing agglomerates of the NP.

We prepared a poly-(ethylene glycol)-*block*-lactide/glycolide copolymer (PEG-PLGA) using emulsion solvent diffusion method. The encapsulated agents are entrapped into the core of PEG-PLGA polymer matrix as shown below.

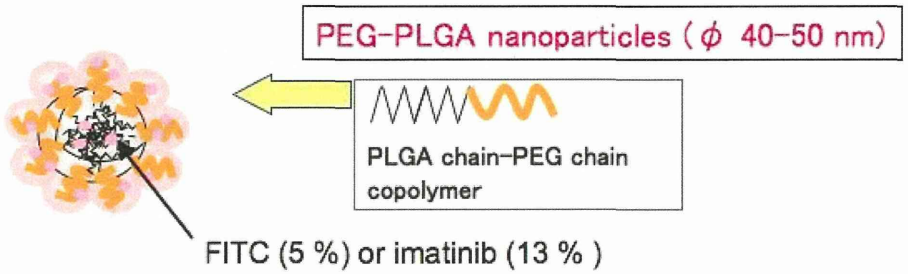

Advantages of PLGA NP-based drug delivery system (DDS) include:

- Matrix polymer (both PEG and PLGA) is bioabsorbable.
- NP can incorporate water-soluble drugs/oligonucleotides/DNAs.
- NP can cross cell membrane via endocytosis (efficiency of cellular uptake: 90 % or more), and deliver the encapsulated agents into the cytoplasm.
- Incorporated drugs are slowly released from NP with hydrolysis of PLGA.

The mean particle size was analyzed by light scattering method (Microtrack UPA150; Nikkiso, Tokyo, Japan). A sample of nanoparticulate suspension in distilled water was used for particle size analysis. An average diameter of PEG-PLGA NP was 44 nm with a narrow size distribution (see Figure in the next page). The FITC-, coumarin-6 and STI571-encapsulated PEG-PLGA NP contained 5 % (w/w) FITC, 3 % (w/w) coumarin-6, and 13 % (w/w) STI571, respectively.

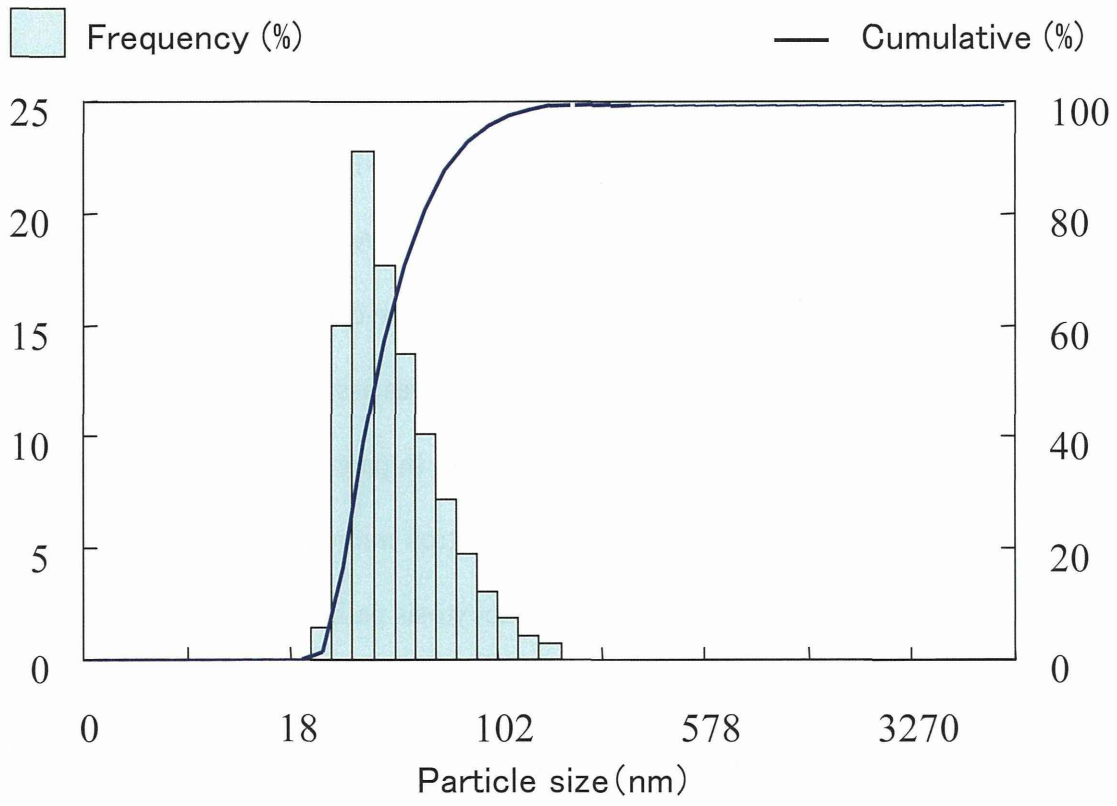

Particle size distribution of FITC-incorporated PEG-PLGA nanoparticles in water

Cellular uptake and intracellular distribution of NP in vitro

Rat aortic smooth muscle cells (SMCs) were obtained from a commercial source (Toyobo) and then cultured in DMEM (Sigma) supplemented with 10 % FBS (Equitech-Bio, Inc.) except where otherwise indicated. Each cells were used between passages 4 to 8. SMCs were seeded on chambered cover glasses and incubated at 37 °C/5 % CO_2 environment until cells were subconfluent. The growth medium was replaced with the coumarin-6- encapsulated PEG-PLGA NP suspension medium (0.5 mg/ml) and then further incubated for 1 hour. At the end of experiment, the cells were washed three times with PBS to eliminate excess NP which were not incorporated into the cells. Then, the cells were fixed with 1 % formaldehyde/PBS buffer and nuclear was counterstained with propidium iodide (PI). Cellular uptake of coumarin-6- encapsulated PEG-PLGA NP was evaluated by fluorescence microscopy. The images were digitized and analyzed with Adobe Photoshop and Scion Image Software. The total number of fluorescence positive cells in each field and the number of total cells was counted. Cellular uptake percentage was assessed by the percentage of fluorescence positive cells per total cells in each field. In part of experiment, the internal properties of NP was examined by transmission electron microscopy (H-7000E, Hitachi, Tokyo, Japan). To confirm NP is uptaken via endocytosis pathway, the chambered cover glasses seeded SMCs were treated with chlorpromazine hydrochloride (CPZ) (Sigma) at 50 μM for 30 minutes[3] and then, with the coumarin-6-encapsulated PEG-PLGA NP-suspension medium (0.05 mg/ml) and then further incubated for 30 minutes. SMCs were fixed and counterstained with PI for fluorescence microscopic study.

Measurement of *in vitro* FITC release kinetics from NP To measure FITC release kinetics, FITC-NP (n = 8) was immersed in Tris-EDTA buffer, and the released FITC from NP was measured.

Cell proliferation, migration, cytotoxicity and TUNEL assay

Human coronary artery SMCs (Lonza. Inc. Walkersville, MD, USA) were cultured, and placed into 48-well culture plates. The cells were stimulated by the addition of PDGF at 10 ng/mL (Sigma, Tokyo, Japan).[4] Either various concentration of STI571 (0.1, 1, 10 μM), STI571-encapsulated PEG-PLGA NP (PEG-PLGA at 0.05 mg/ml containing STI571 at 10 μM), or vehicle alone was added to the wells, and four days later, the cells were fixed with methanol and stained with Diff-Quick staining solution (Sysmex corporation, Kobe, Japan) and a single observer counted the number of cells/plate.

Migration of rat aortic SMCs was assessed with a Boyden chamber type cell migration assay kit housing a collagen-precoated polycarbonate membrane with 8.0-μm pores (Chemicon international Inc.), as we previously described[5]. Lower chambers were filled with solvent or human PDGF at 10 ng/mL. Then cells (1×10^5 cells/mL) were placed on the upper side of the membrane and allowed to migrate through the pores. STI571 (0.1, 1, 10 μM), STI571-encapsulated PEG-PLGA NP (PEG-PLGA at 0.05 mg/ml containing STI571 at 10μM), or vehicle alone was added to the upper chamber. After 4 hours of incubation, the number of cells that migrated to the lower surface of the membrane was counted per x 200 high-power fields.

The cytotoxicity of PEG-PLGA NP on human coronary artery SMCs was determined using a MTS assay (Cell Counting Kit-8, Dojindo Inc.). The cells were grown in 96-well microtiter plates for 24 hours, and then they were treated with different concentrations of FITC-incorporated PEG-PLGA NP suspension medium with 10 % FBS. The plates were incubated for 48 hours and then the medium was replaced with 200 μl of fresh medium. Next, 2 mg/ml MTS solution was added and the plates were incubated again for 4 hours at 37°C/5%CO_2. Finally, absorbance was measured at 490 nM using microplate reader. Cell viability was expressed as the ratio between the amount of formazan determined for cells treated with PEG-PLGA NP and for control non-treated cells.

Apoptotic cells were detected by terminal deoxynucleotidyl transferase-mediated dUTP nick end-labeling (TUNEL) staining (in situ apoptosis detection kit, Takara).

Experimental animal models

All *in vivo* experiments were reviewed and approved by the Committee on Ethics on Animal Experiments, Kyushu University Faculty of Medicine, according to the Guidelines of the American Physiologic Society.

Male Japanese white rabbits (KBT Oriental, Tokyo) weighting 2.5 to 3.0 kg, were fed a high cholesterol diet containing 1% cholesterol and 3% peanut oil for 2 weeks before the operation. Animals were anesthetized with intramuscularly injection with ketamine hydrochloride (50 mg/kg) and xyradine (10 mg/kg), and a midline neck incision was made to expose the left jugular vein and the left common carotid artery. An approximately 3-cm segment of the jugular vein was dissected free using a non-touch technique, and all side branches were ligated with 4-0 silk ties. The vein segments were gently flushed to remove residual blood, and placed in a buffer alone (n = 11) or in a solution containing either FITC-encapsulated PEG-PLGA NP at 0.5 mg/ml (n = 11), STI571- encapsulated PEG-PLGA NP at 0.5 mg/ml containing STI571 at 100 μM (n = 11), or and STI571 alone at 100 μM (n = 11) for 30 minutes at room temperature. The treated vein segments were interposed into ipsilateral carotid arteries in an end-to-side fashion with 7-0 polypropylene monofilament sutures after intravenous heparin at 1000 IU. The animals were maintained on the same high cholesterol diet throughout experimental period.

All animals received aspirin at 20 mg/day until euthanasia from 3 days before the graft procedure. After venous blood samples were taken, animals were killed with a lethal dose of anesthesia on days 7 (n =5 each) and 28 (n =6 each). The vein grafts were harvested, flushed with saline and divided into two parts at the center of the segment. The proximal part was used for histopathological and immunohistochemical study. The distal part was snap-frozen

in liquid nitrogen and stored at -70 °C used for Western blotting analyses.

***Ex vivo* NP delivery in human vein**

Segments of internal thoracic vein were obtained from patients undergoing coronary arterial bypass surgery. Ethical permission was obtained from the ethical committee of Kyushu University. The vein segments were incubated *ex vivo* with FITC- encapsulated PEG-PLGA NP at 0.5mg/ml for 30 minutes at room temperature. Cellular uptake of FITC was evaluated by fluorescence microscopy.

Histopathological and Immunohistochemical Study

Tissue sections from the grafts were prepared and either stained with Elastica Van Gieson. The neointimal area, the area within the internal elastic lamina (IEL), and the lumen area were measured by computerized morphometry, which was carried out by a single observer who was blinded to the experimental protocol. The sections were also subjected to immunohistochemical staining using with either non-immune mouse IgG (Dako) as a control, or with antibodies against PDGF-B (PGF-007, Mochida), macrophage (RAM-11, 1:100), proliferating cells (PCNA, 1:50), endothelial cells (CD31, 1:50, all from DAKO, Tokyo, Japan), and FITC (American Reserarch Product, Belmont, MA, 1:1000). Following avidin-biotin amplification, the slides were incubated with diaminobenzidine and counterstained with hematoxylin. To quantify proliferating cells, at least four representative images were collected, and the percentage of PCNA-positive cells per total cells in each picture was calculated; the average of the four pictures was reported for each animal. The percentage of total areas of positive cells with PDGF-B, macrophage, and FITC in each section was measured. Endothelial cell coverage was also quantified followed by the formula: 100 x (the length of CD31-positive layer / the length of luminal surface in cross-sections). All images were captured by an Olympus microscope equipped with a digital camera (HC-2500) and were analyzed using Adobe Photoshop CS and Scion Image

Software.

Western blot analysis

Protein was extracted from cultured vascular SMCs or frozen vein graft tissues. Samples were homogenized in lysis buffer containing 10 mM Tris-HCl, pH 7.4, 50 mM NaCl, 5 mM EDTA, 1 % Triton X-100, 50 mM NaCl, 30 mM sodium phosphate, 50 mM NaF, 1 % aprotinin, 0.5 % pepstatin A, 2 mM phenylmethylsulfonyl fluoride, and 5 mM leupeptin and phosphatase inhibitor cocktail (Pierce, Rockford, IL). Cell lysates (20 μg) were separated on 7.5 % polyacrylamide gels and blotted onto polyvinylidene difluoride membranes (Millipore Co. Hercules, Ca). Protein expression was analyzed using antibodies against human PDGF-R-β (0.1 mg/ml), phospho-PDGF-R-β (0.5 mg/ml), ERK 1/2 (0.5 μg/ml, all from R&D Systems Inc., MN), phosphotyrosine (0.5 μg/ml, clone 4G10, Upstate), phosho-p44/42 MAPK (1:2000, Cell Signaling), c-Abl TK (0.1 μg/ml, Santa Cruz Biotechnology Inc.), or actin (Sigma). Immune complexes were visualized with horseradish peroxidase–conjugated secondary antibodies. Bounded antibodies were detected by chemiluminescence with the use of an ECL detection system (Amersham Biosciences) and quantified by densitometry.

Cytotoxicity and TUNEL assays

The cytotoxicity of PEG-PLGA NP on human coronary artery SMCs was determined using a MTS assay (Cell Counting Kit-8, Dojindo Inc., #343-07626). The cells were grown in 96-well microtiter plates for 24 hours, and then they were treated with different concentrations of FITC-encapsulated PEG-PLGA nanoparticles NP suspension medium with 10 % FBS. The plates were incubated for 48 hours and then the medium was replaced with 200 μl of fresh medium. Next, 2 mg/ml MTS solution was added and the plates were incubated again for 4 hours at 37°C/5%CO_2. Finally, absorbance was measured at 490 nM using an enzyme-linked immunosorbent assay microplate reader. Cell viability

was expressed as the ratio between the amount of formazan determined for cells treated with PEG-PLGA nanoparticles NP and for control non-treated cells.

Apoptotic cells were detected by terminal deoxynucleotidyl transferase-mediated dUTP nick end-labeling (TUNEL) staining (in situ apoptosis detection kit, Takara).

Statistical Analysis

Data are expressed as the mean ± SE. Statistical analysis of differences was compared by ANOVA and Bonferroni's multiple comparison tests. A level of $P < 0.05$ was considered statistically significant.

References

1. Murakami H, Kobayashi M, Takeuchi H, Kawashima Y. Preparation of poly(DL-lactide-co-glycolide) nanoparticles by modified spontaneous emulsification solvent diffusion method. *International journal of pharmaceutics.* 1999;187(2):143-152.

2. Kawashima Y, Yamamoto H, Takeuchi H, Hino T, Niwa T. Properties of a peptide containing DL-lactide/glycolide copolymer nanospheres prepared by novel emulsion solvent diffusion methods. *Eur J Pharm Biopharm.* 1998;45(1):41-48.

3. Wang LH, Rothberg KG, Anderson RG. Mis-assembly of clathrin lattices on endosomes reveals a regulatory switch for coated pit formation. *The Journal of cell biology.* 1993;123(5):1107-1117.

4. Nakano K, Egashira K, Tada H, Kohjimoto Y, Hirouchi Y, Kitajima S, Endo Y, Li XH, Sunagawa K. A third-generation, long-acting, dihydropyridine calcium antagonist, azelnidipine, attenuates stent-associated neointimal formation in non-human primates. *J Hypertens.* 2006;24(9):1881-1889.

5. Ono H, Ichiki T, Fukuyama K, Iino N, Masuda S, Egashira K, Takeshita A. cAMP-response element-binding protein mediates tumor necrosis factor-alpha-induced vascular smooth muscle cell migration. *Arterioscler Thromb Vasc Biol.* 2004;24(9):1634-1639.

Figure I. Effects of an endocytosis inhibitor chlorpromazine hydrochloride (CPZ) on NP-mediated intracellular incorporation of fluorescence

Fluorescence microscopic pictures of rat aortic SMCs incubated with coumarin-6--encapsulated PEG-PLGA NP (0.05 mg/ml) for 30 minutes in the presence and absence of chlorpromazine hydrochroride (CPZ) at 50 μM. The Nuclei were counterstained with propidium iodide (PI). Scale bar = 50 μm

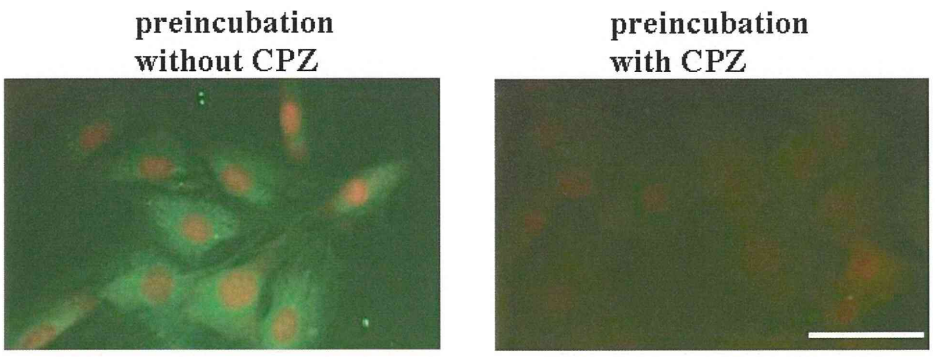

Figure II. Efficacy of NP-mediated drug delivery system to vein grafts

A, Fluorescence micrographs of cross-sections of excised rabbit jugular vein and human internal thoracic vein after *ex vivo* incubation with PBS or FITC-NP for 30 minutes. FITC fluorescence is green. Nuclei are stained red. M: media, A: adventitia. Scale bar = 100 μm

B, Micrographs of cross-sections of excised rabbit jugular vein stained with FITC antibody immediately after *ex vivo* incubation with FITC-NP, and at 7 and 28 days after implantation. The nuclei are counterstained with hematoxylin. M: media, IM: intima + media complex, A: adventitia. White line shows external elastic lamina. Scale bar = 100 μm

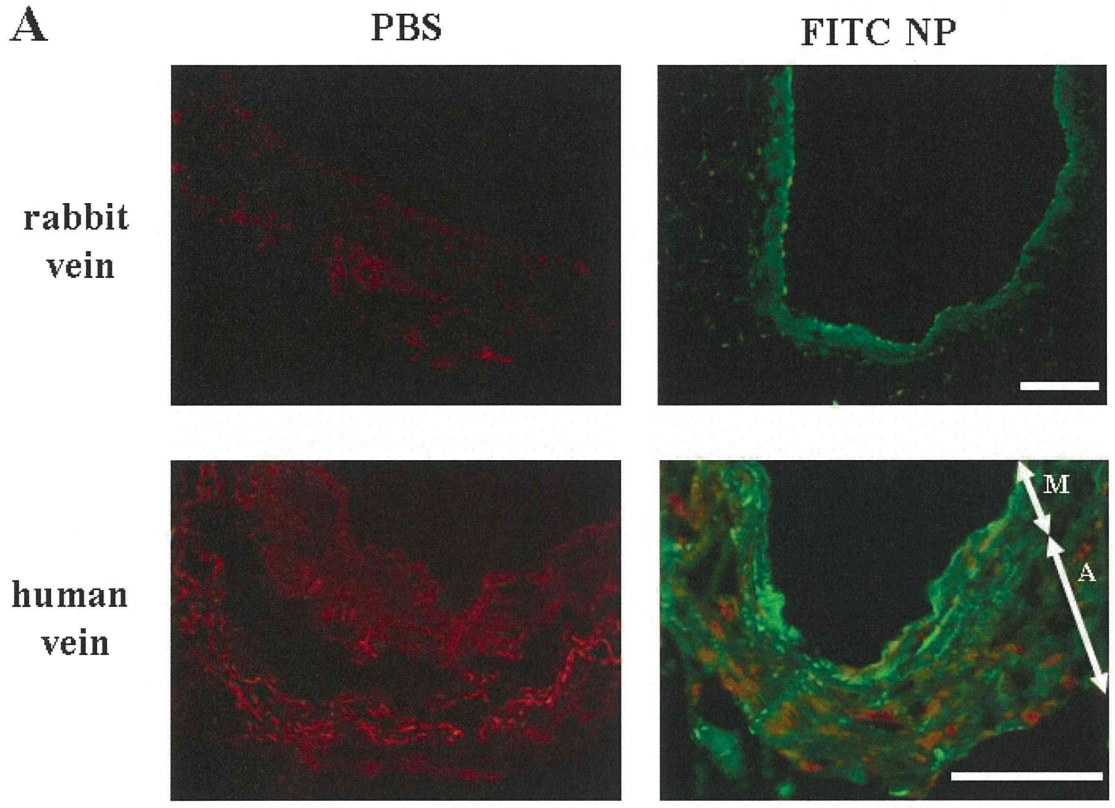

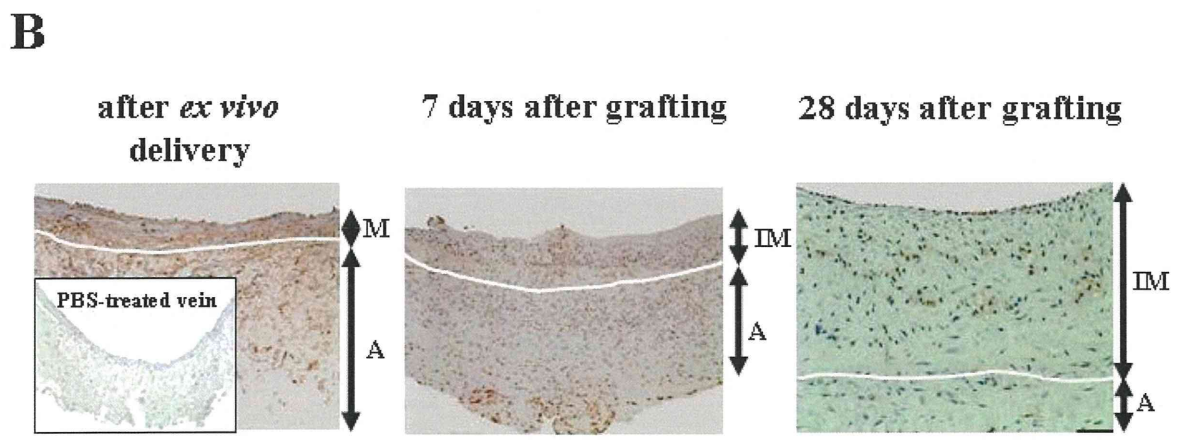

Figure III. Effects of NP-based STI571 delivery on inflammatory and proliferative changes, and endothelial regeneration

A, Pictures of cross-sections of vein grafts 7 days after implantation, stained to detect monocytes/macrophages (RAM-11), proliferating cells (PCNA), and endothelial cells (CD31). IM: intima + media complex; A: adventitia. White line shows external elastic lamina. Bar = 50 μm

B, Summary data on inflammation

C, Summary data on the appearance of PCNA-positive cells

D, Summary data on endothelial regeneration. Endothelial cell coverage was quantified by the following formula: 100 × (the length of CD31-positive layer / the length of luminal surface in cross-sections). $^{**}P < 0.01$ versus PBS-treated group, NS; Not significant.

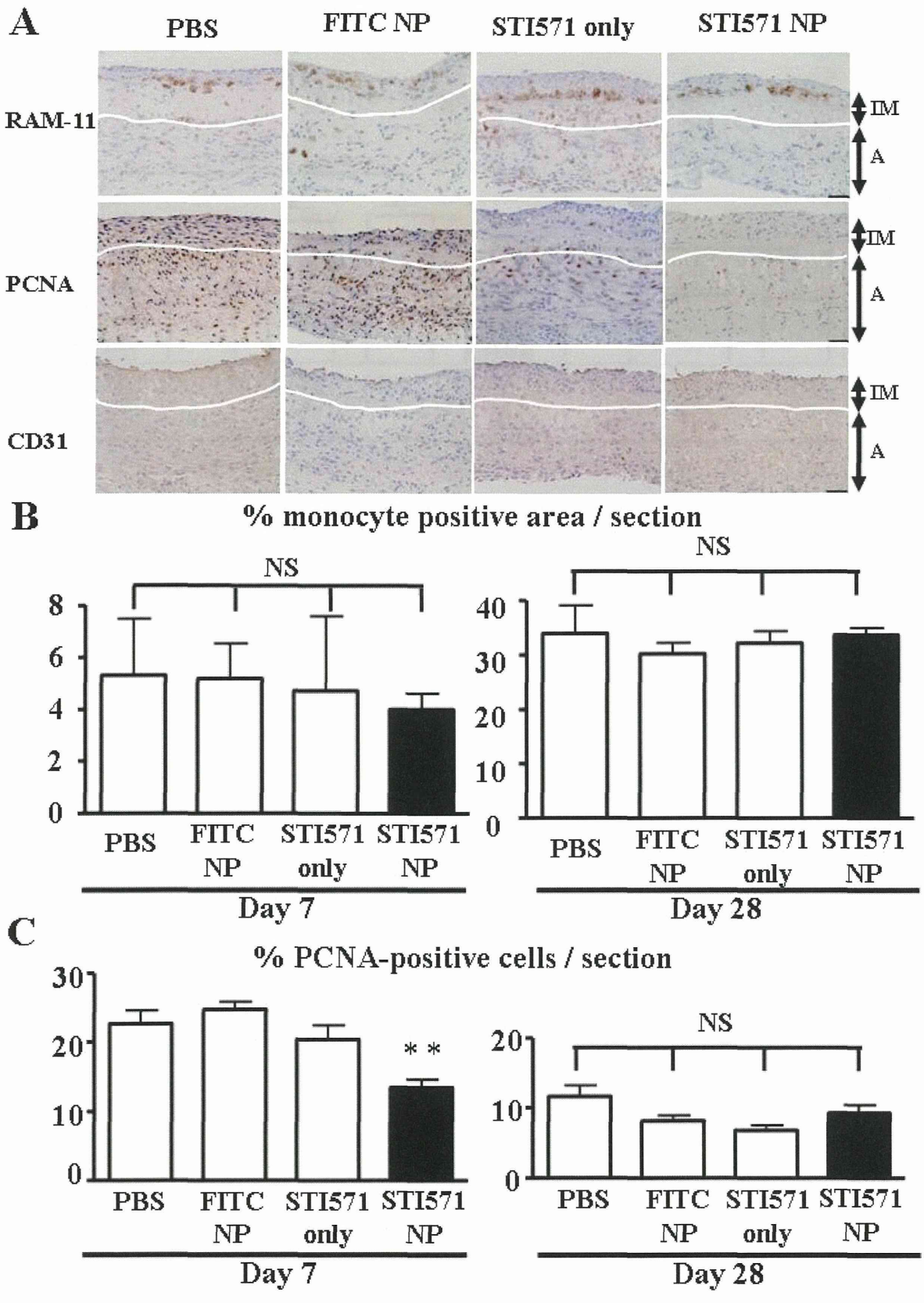

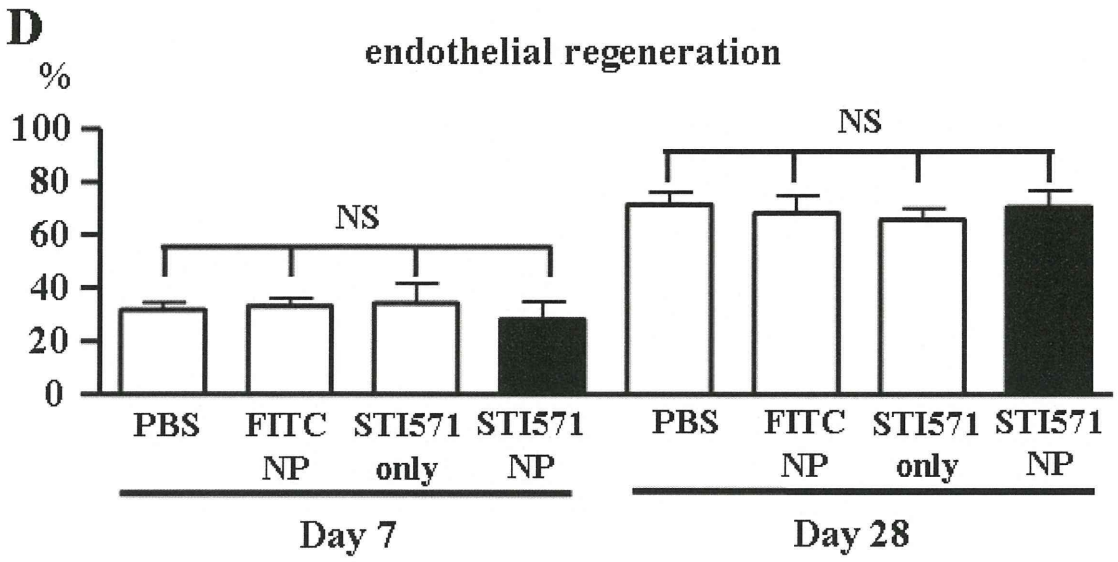

Figure IV. Effects of STI571-NP on PDGF expression

A, Photomicrographs of cross-sections of vein immunohistochemically stained for PDGF from normal vein and vein graft tissues 7 days after grafting. Lower photomicrographs of cross sections is magnified in box of upper image. Scale bar in low- and high-powered field = 100 and 50 μm

B, Percentage of PDGF-positive cells in PBS, FITC-NP, STI571 only, and STI571-NP groups (n = 5 each). There was no treatment effect. Data are mean ± SEM. NS; Not significant.